Molecular Biology of the Cell
Vol. 21, 1725–1736, May 15, 2010

Roles of the Mdm10, Tom7, Mdm12, and Mmm1 Proteins in the Assembly of Mitochondrial Outer Membrane Proteins in *Neurospora crassa*

Jeremy G. Wideman,* Nancy E. Go,* Astrid Klein,† Erin Redmond,* Sebastian W.K. Lackey,* Tan Tao,‡ Hubert Kalbacher,‡ Doron Rapaport,‡ Walter Neupert,† and Frank E. Nargang*

*Department of Biological Sciences, University of Alberta, Edmonton, Alberta T6G 2E9, Canada; †Institut für Physiologische Chemie, Universität München, D-81377 München, Germany; and ‡Interfaculty Institute for Biochemistry, University of Tübingen, 72076 Tübingen, Germany

Submitted October 2, 2009; Revised February 2, 2010; Accepted March 11, 2010
Monitoring Editor: Thomas D. Fox

The Mdm10, Mdm12, and Mmm1 proteins have been implicated in several mitochondrial functions including mitochondrial distribution and morphology, assembly of β-barrel proteins such as Tom40 and porin, association of mitochondria and endoplasmic reticulum, and maintaining lipid composition of mitochondrial membranes. Here we show that loss of any of these three proteins in *Neurospora crassa* results in the formation of large mitochondrial tubules and reduces the assembly of porin and Tom40 into the outer membrane. We have also investigated the relationship of Mdm10 and Tom7 in the biogenesis of β-barrel proteins. Previous work showed that mitochondria lacking Tom7 assemble Tom40 more efficiently, and porin less efficiently, than wild-type mitochondria. Analysis of *mdm10* and *tom7* single and double mutants, has demonstrated that the effects of the two mutations are additive. Loss of Tom7 partially compensates for the decrease in Tom40 assembly resulting from loss of Mdm10, whereas porin assembly is more severely reduced in the double mutant than in either single mutant. The additive effects observed in the double mutant suggest that different steps in β-barrel assembly are affected in the individual mutants. Many aspects of Tom7 and Mdm10 function in *N. crassa* are different from those of their homologues in *Saccharomyces cerevisiae*.

INTRODUCTION

The TOB (topogenesis of mitochondrial outer membrane β-barrel proteins) complex, which is also known as the SAM (sorting and assembly machinery) complex, contains three core components: Tob55 (Sam50, Omp85), Tob38 (Tom38, Sam35), and Mas37 (Sam37, Tom37), which we will refer to as Tob37 in the *Neurospora crassa* TOB complex. The major function of the complex is to integrate β-barrel proteins (Tom40, porin, Tob55, Mdm10, and Mmm2) into the outer mitochondrial membrane, although assembly of a few non β-barrel outer membrane proteins is also dependent on TOB complex components (reviewed in Neupert and Herrmann, 2007; Becker *et al.*, 2008, 2009; Bolender *et al.*, 2008; Chacinska *et al.*, 2009; Walther *et al.*, 2009). Four other proteins have been shown to play a role in mitochondrial β-barrel protein assembly in *Saccharomyces cerevisiae* in steps that follow the action of the TOB complex. Mdm12 and Mmm1 are required on the general insertion pathway for all β-barrel proteins (Meisinger *et al.*, 2007), whereas Mdm10 (Meisinger *et al.*, 2004) and Mim1 (Ishikawa *et al.*, 2004; Waizenegger *et al.*, 2005; Lueder and Lithgow, 2009) participate specifically in Tom40 assembly.

Mdm10, Mdm12, and Mmm1 may have diverse roles as they were originally described as mitochondrial proteins required for proper mitochondrial distribution and the maintenance of mitochondrial morphology. The three proteins were shown to exist in a complex that was thought to be involved in mtDNA segregation in *S. cerevisiae* (Boldogh *et al.*, 2003). Knocking out the genes encoding these proteins was found to result in the formation of giant mitochondria accompanied by various growth defects in *S. cerevisiae*. Mutants lacking Mdm10 grew slowly at 23°C and not at all at 37°C. Even at permissive temperatures, almost all cells were found to contain only giant mitochondria (Sogo and Yaffe, 1994; Meisinger *et al.*, 2006). *S. cerevisiae* cells lacking Mmm1 grew slowly and contained only giant mitochondria at both 23 and 37°C (Burgess *et al.*, 1994). Loss of Mdm12 gave cells that grew slowly at 23°C and were unable to grow at 37°C, with large spherical mitochondria present at both temperatures (Berger *et al.*, 1997). Mutations in the homologues of these genes in other organisms give rise to related but not always identical growth and morphological phenotypes. Deletion of the *mdm10* gene in *Aspergillus nidulans* resulted in a strain that grew at the same rate as wild type at 37°C, but

This article was published online ahead of print in *MBoC in Press* (http://www.molbiolcell.org/cgi/doi/10.1091/mbc.E09–10–0844) on March 24, 2010.

Address correspondence to: Frank E. Nargang (frank.nargang@ualberta.ca).

Abbreviations used: AAC, ADP/ATP carrier; BNGE, blue native gel electrophoresis; $F_1\beta$, β-subunit of the F_1 ATP synthase; Ni-NTA, Ni-nitrolotriacetic acid; OMV, outer membrane vesicles; PMSF, phenylmethylsulfonyl fluoride; SAM, sorting and assembly machinery; SEMP, 0.25 M sucrose, 10 mM MOPS, pH 7.2, 1 mM EDTA, and 1 mM PMSF; TOB, topogenesis of mitochondrial outer membrane β-barrel proteins; TOM, translocase of the outer mitochondrial membrane.

grew slightly slower at 20°C. Mitochondria existed as identical tubular networks in both mutant and wild-type cells grown at 37°C, but in mutant cells grown at 20°C more than 90% of hyphal compartments contained some large circular mitochondria in addition to normal tubular mitochondria (Koch *et al.*, 2003). An *mdm10* missense mutant of *Podospora anserina* grew more slowly than wild type at 35°C, and all mitochondria were enlarged. No differences in growth or mitochondrial morphology were seen at 18°C (Jamet-Vierny *et al.*, 1997). A *Neurospora crassa mmm1* mutant produced by repeat induced point mutation was inviable at 40°C and grew slowly at 21, 30, or 37°C. Giant long mitochondria were observed in hyphae, and giant circular mitochondria were seen in conidiaspores (Prokisch *et al.*, 2000). The variation in phenotypes among different organisms suggests that the functions of the proteins may be slightly different in different species or that some organisms may contain other proteins with a degree of functional overlap.

The diverse roles of Mdm10, Mdm12, and Mmm1 were recently extended by the finding that these proteins exist in a complex, together with Mdm34, that acts as a tether between the endoplasmic reticulum (ER) and mitochondria. It was suggested that the connection allows the two organelles to exchange phospholipids and calcium (Kornmann *et al.*, 2009). Localization studies identified Mdm10 and Mdm34 as mitochondrial proteins but, contrary to previous findings, Mmm1 was found to be a protein of the ER. Mdm12 was found to be a peripheral membrane protein that was capable of interaction with both the ER and mitochondrial components of the complex (Kornmann *et al.*, 2009).

Although Mdm10, Mdm12, and Mmm1 have been implicated in a variety of functions, it has not been definitively shown whether they are multifunctional proteins or if loss of a primary function results in secondary phenotypic effects. Because there are different possibilities for the function and mechanism of action of these proteins, we wanted to determine if Mdm10, Mdm12, and Mmm1 affected the assembly of β-barrel proteins into the mitochondrial outer membrane of another organism, *N. crassa*. In addition, we have examined the relationship of Mdm10 and Tom7 in the assembly of Tom40 and porin. During the study of *S. cerevisiae* mutants lacking Mdm10 it was observed that a decrease in Tom40 assembly was accompanied by an increased efficiency of porin assembly (Meisinger *et al.*, 2004). Interestingly, the opposite effects on the rate of assembly of Tom40 and porin have been described in Tom7 mutants of both *S. cerevisiae* and *N. crassa* (Meisinger *et al.*, 2004; Sherman *et al.*, 2005). To explore further the relationship between Mdm10 and Tom7 function in the assembly of these β-barrel proteins, we have analyzed assembly in single and double *mdm10* and *tom7* mutants.

MATERIALS AND METHODS

Strains and Growth of N. crassa

The strains used in this study are shown in Table 1. Growth, crossing and general handling of *N. crassa* strains were as described previously (Davis and De Serres, 1970).

Antibody Production

An antibody to *N. crassa* Mdm10 was prepared by injecting guinea pigs with a fusion protein composed of hexahistidinyl-tag, mouse dihydrofolate reductase, and residues 5-298 of the *N. crassa* Mdm10 protein. The sequence encoding the fusion protein was constructed in pQE40 (QIAGEN, Mississauga, ON, Canada). After expression in *Escherichia coli*, the fusion protein was purified on a Ni-NTA (Ni-nitrolotriacetic acid) column (QIAGEN) in 8 M urea according to the manufacturer's instructions except that the protein was eluted in 0.1% SDS, 10 mM Tris-HCl, pH 7.4. The eluate was injected into guinea pigs and mice without further processing. Antibodies to *N. crassa* Tob37 and Tob38 were raised using various approaches. For Tob37, a peptide corresponding to residues 305-319 (TFPDSGKVLPWADRE) of the protein was injected into guinea pigs and mice. Peptides corresponding to residues 165-184 (DTDAEMERLEREEREREAAG), 212-233 (KRRIKLEGLAAEVFDVLGEVDF), and 426-442 (VGLGSFGAAGAMFAGLA) were injected into rabbits. For Tob38, the region coding residues 1-185 of the protein was cloned into pQE40 to give a gene encoding a fusion protein consisting of a hexahistidinyl-tag, mouse dihydrofolate reductase, and *N. crassa* Tob38 (residues 1-185). The fusion protein was purified as described above for the Mdm10 fusion protein and injected into guinea pigs and mice. In addition, peptides corresponding to residues 164-182 (RDPEYTDLLDRFYITPASS) and 269-290 (KYMSDAEGEVEGNMGFILASRK) were injected into rabbits. The *N. crassa* Mim1 antibody was raised against a peptide containing residues 109-123 (VVERPRRRVDLDDHL) of the protein and was injected into rabbits.

All peptide antigens were coupled to KLH (keyhole limpet hemocyanin) before injection. For all antisera, the first injection was done in the presence of either Freund's complete adjuvant or Titer Max Gold (Sigma, München, Germany). Boosters were given in the presence of Freund's incomplete adjuvant.

Table 1. Strains used in this study

Strain	Genotype	Origin or source and reference (if applicable)
NCN251	A	FGSC[a] 2489
76-26	*his-3 mtrR a*	R. L. Metzenberg
Δ *mdm10*	Δ *mdm10 his-3 mtrR hygR a*	Replacement of *mdm10* gene in 76-26 with hygromycin resistance (HygR) cassette
Δ *tom7*	Δ *tom7 hygR A*	Nargang lab (Sherman *et al.*, 2005)
Δ *mdm10*Δ *tom7*	Δ *tom7* Δ *mdm10 hygR*	Cross of Δ*mdm10* with Δ *tom7*
mdm12	*mdm12*	FGSC 9852 (Seiler and Plamann, 2003)
mmm1-RIP23	$mmm1^{RIP}$	Neupert lab (Prokisch *et al.*, 2000)
His9-Tob55 (H6C4-5)	*his-3 mtrR a* Δ *tob55 hygR* Contains an ectopic copy of genomic *tob55* with an N-terminal nine His tag. Also bleomycin resistant.	Nargang lab
His9-Tob37 (9His-Tob37-2)	*his-3 mtrR a* Δ *tob37 hygR* Contains an ectopic copy of genomic *tob37* with a C-terminal nine His tag. Also bleomycin resistant.	Nargang lab
His9-Tob38 (9His-Tob38-3)	*his-3 mtrR a* Δ *tob38 hygR* Contains an ectopic copy of genomic *tob38* with a C-terminal nine His tag. Also bleomycin resistant.	Nargang lab

[a] Fungal Genetics Stock Center.

Fluorescence Microscopy of Mitochondria

Examination of mitochondria in hyphae was done using a previously described method (Hickey *et al.*, 2005) with modifications. Conidia were inoculated in the center of Petri plates containing a thin layer of medium (~1 mm thick) that was solidified with agarose. The plates were incubated at 30°C for 6–8 h. After incubation 20 μl of 500 nM MitoTracker Green (Molecular

Probes, Eugene, OR) in liquid medium was applied to the hyphal tips of the growing mycelium. Incubation was allowed to continue for an additional 30 min. Using a scalpel, agarose blocks containing growing hyphal tips were cut and placed on a microscope slide, covered with a coverslip, and visualized by epifluorescent microscopy. Samples were viewed using a Planapochromat 63× oil immersion objective (1.4 NA; working distance, 0.19 mm) of an AxioImager M1 (Carl Zeiss, Oberkochen, Germany) equipped with an ORCA-ER digital camera (Hamamatsu Photonics K.K., Hamamatsu, Japan). MitoTracker Green was visualized using a 50% attenuated HBO103 mercury vapor short-arc lamp (Osram, München, Germany), with a BP470/40 excitation filter, an FT 495 beam splitter and a BP525/50 emission filter (Carl Zeiss). A higher dye concentration than generally recommended (500 nM rather than 20–200 nM) was used to account for diffusion into the surrounding media. Images were cropped and adjusted for brightness and contrast in Adobe Photoshop (San Jose, CA).

Measuring Mitochondrial Diameter and Statistical Analysis

The diameter of 50 mitochondrial tubules from each strain were measured using ImageJ (National Institutes of Health, http://rsb.info.nih.gov/ij). The average diameter and SD for mitochondria of each strain were calculated.

Isolation of Mitochondria, Alkaline Extraction, and Preparation of Whole Cell Extracts

Unless specified otherwise, mycelia were grown at 30°C, harvested by filtration, and ground in the presence of sand and SEMP isolation buffer (0.25 M sucrose, 10 mM MOPS, pH 7.2, 1 mM EDTA,1 mM phenylmethylsulfonyl fluoride [PMSF]) using a mortar and pestle. Mitochondria were isolated by differential centrifugation as described (Nargang and Rapaport, 2007). To determine if proteins were integral membrane proteins, alkaline extraction was performed. Mitochondria (50 μg protein) were suspended in 1 ml of 0.1 M sodium carbonate (pH 11.0) on ice for 30 min. The mixture was then centrifuged at 50,000 rpm in a TLA55 rotor (Beckman Instruments, Palo Alto, CA) at 2°C for 30 min. The pellets were processed for electrophoresis. Proteins in the supernatant were precipitated in the presence of 7% trichloroacetic acid, centrifuged as described above, washed with acetone, dried, and processed for electrophoresis.

Whole cell extracts were prepared by grinding mycelia in the presence of sand and protein isolation buffer (10 mM MOPS, pH 7.2, 1 mM EDTA, 1% SDS, 1 mM PMSF) followed by centrifugation (3000 × *g*, 20 min, 4°C) to remove cellular debris. The supernatant was further clarified by centrifugation (12000 × *g*, 20 min, 4°C) to produce the whole cell extract and then assayed for protein concentration using the BCA-200 protein assay system (Pierce, Rockford, IL).

Preparation of Damaged Mitochondria

To create mitochondria from wild-type cells that were similar to those isolated from strains containing enlarged mitochondria, we used a modified osmotic shock treatment. Isolated wild-type mitochondria in SEMP buffer (500 μg of mitochondrial protein) were pelleted by centrifugation (16000 × *g*, 15 min, 4°C), resuspended in 1 ml of swelling buffer (1 mM KPO_4, 1 mM EDTA, pH 7.2), and incubated on ice for 30 min. Every 5 min the mitochondria were vortexed at high speed for 10 s. Mitochondria were reisolated by centrifugation (16000 × *g*, 15 min, 4°C) and resuspended in fresh SEMP. We refer to the mitochondria obtained by this treatment as "damaged" mitochondria.

Affinity Purification on Ni-NTA Columns

Mitochondria were isolated, as described above, from strains expressing nine His-tagged versions of Tob37, Tob38, or Tob55 rather than the wild-type proteins. Sample preparation and Ni-NTA chromatography was performed as described previously (Meisinger *et al.,* 2004) except that 20 mM imidazole was included during binding of complexes to the Ni-NTA resin. Proteins in the collected fractions were precipitated in 15% trichloroacetic acid, washed with acetone, and then subjected to SDS PAGE and Western blotting.

Phospholipid Analysis

Outer membrane vesicles (OMV) were prepared from isolated mitochondria as described previously (Mayer *et al.,* 1995). Phospholipids were extracted from OMVs by adding 100 μl of a 2:1 (vol/vol) chloroform/ethanol mixture to a suspension of OMVs in 100 μl of water. Samples were vortexed and then centrifuged to separate the aqueous phase from the organic phase, which contained the lipids. The organic solvents were evaporated and lipids were dissolved in 100 μl 2:1 (vol/vol) chloroform/ethanol. Phosphate determination (Böttcher *et al.,* 1961) and analysis of phospholipids by thin-layer chromatography (TLC) were as previously described (Vaden *et al.,* 2005) except that lipids were detected by staining the dried TLC plates with molybdenum blue.

Standard Procedures

Blue native gel electrophoresis (BNGE; Schägger and von Jagow, 1991; Schägger *et al.,* 1994), Western blotting (Good and Crosby, 1989), and import of precursor proteins into isolated mitochondria (Harkness *et al.,* 1994) were performed as described previously. In some figures, irrelevant lanes were removed electronically.

RESULTS

Mutant Construction and Mitochondrial Morphology in **mdm10** *and* **tom7** *Mutant Strains*

We identified the NCU07824 protein as the homolog of the *S. cerevisiae* Mdm10 protein from the *N. crassa* genome sequence (Galagan *et al.,* 2003). Comparisons of the protein predicted at the *N. crassa* database (http://www.broadinstitute.org/annotation/genome/neurospora/MultiHome.html) with that of *S. cerevisiae* revealed the existence of large regions containing little sequence similarity. This prompted us to examine 20 *N. crassa mdm10* cDNAs because of the possibility that introns were misidentified in the genome sequence. Comparison of the cDNAs to the predicted genomic coding sequence showed that one region near the C-terminus was predicted to be an intron but was found to be present in all 20 cDNAs. Another region that encoded 24 amino acid residues near the N-terminus was included in the predicted coding sequence but was found in only two of the 20 cDNAs. Thus, this sequence is removed as an intron in the majority of transcripts, but a low level of alternative splicing appears to occur in the *mdm10* transcript. The major cDNA would give rise to a 480-amino acid *N. crassa* protein. When this sequence was compared with the 493-amino acid yeast Mdm10 protein it was found to be 27% identical and 48% similar (Supplementary Figure 1).

We constructed a knockout of the *N. crassa mdm10* gene in a sheltered heterokaryon using a hygromycin resistance cassette to replace the *mdm10* coding sequence (Nargang and Rapaport, 2007). Subsequent analysis of conidiaspores produced by the heterokaryon showed that the gene was not essential and a homokaryotic strain in which the *mdm10* gene had been replaced by hygromycin resistance was isolated from the heterokaryon for further experiments. We refer to this strain as Δ*mdm10*. Replacement of the *mdm10* gene was demonstrated by Southern analysis (unpublished observations). We also constructed an Δ*mdm10* Δ*tom7* double mutant by crossing Δ*mdm10* with our previously described Δ*tom7* strain (Sherman *et al.,* 2005) so that we could examine the combined effects of these two mutations on the assembly of β-barrel proteins. Western blots of mitochondria isolated from the single and double mutants revealed the lack of Mdm10 (Figure 1A). We do not have an antibody against *N. crassa* Tom7, but the deletion of the *tom7* gene was demonstrated by PCR analysis of genomic DNA (Figure 1A). *N. crassa* Mdm10 was found to be located in mitochondrial OMV and exhibited behavior similar to Tom40 after alkaline extraction of mitochondria (Figure 1B). We conclude that *N. crassa* Mdm10 is an integral protein of the mitochondrial outer membrane.

Mutations affecting the Mdm10 protein are known to result in the formation of giant mitochondria in various organisms and mitochondria in *S. cerevisiae* strains lacking Tom7 have been shown to have a similar morphological phenotype (Dimmer *et al.,* 2002; Meisinger *et al.,* 2006). We examined our *N. crassa* mutants by fluorescence microscopy after growth at 30°C and staining with MitoTracker Green. Although circular giant mitochondria were not present in Δ*mdm10* mutant cells, we did observe that cells lacking Mdm10 contained tubular mitochondria that were larger in

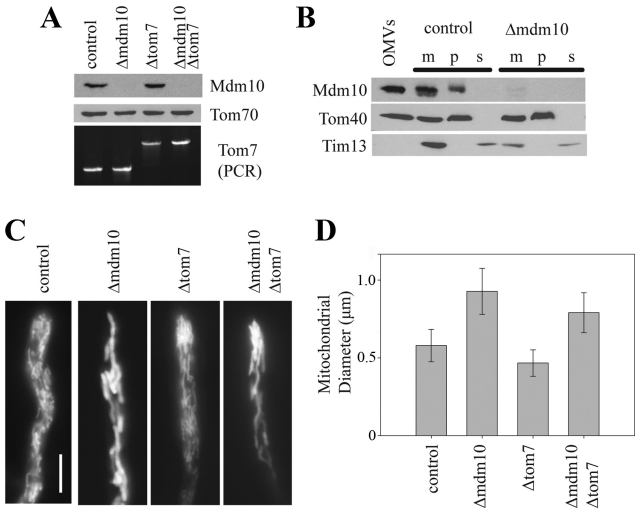

Figure 1. Mdm10 in *N. crassa* and mitochondrial morphology in strains lacking the protein. (A) The top and middle rows show Western blots of mitochondria isolated from the control strain (76-26) and the indicated mutant strains decorated with antibodies to the indicated proteins. The lower panel shows ethidium bromide stained PCR products obtained from genomic DNA of the indicated strains using primers flanking the *tom7* gene. The knockout allele contains a larger product because the disrupting hygromycin cassette is larger than the *tom7* gene that it has replaced. (B) Alkaline extraction of proteins from mitochondria isolated from a control strain (76-26) and the Δ*mdm10* mutant. Isolated mitochondria were resuspended in 0.1 M sodium carbonate (pH 11.0) and incubated on ice for 30 min. Membrane sheets were pelleted (p) by centrifugation and proteins in the supernatant (s) were precipitated with trichloroacetic acid. The fractions were subjected to SDS-PAGE, blotted to nitrocellulose, and immunodecorated with the indicated antibodies. Untreated mitochondria (m) from each strain, and OMV from a control strain (76-26) were included as controls. (C) The indicated strains were grown on a thin layer of solid medium, stained with MitoTracker Green, and hyphal tips were examined by fluorescence microscopy. The bar in the control picture indicates 10 μm. (D) The diameter of mitochondrial tubules was measured in photographs of each of the different strains. Fifty tubules were measured for each strain, and the average diameter was calculated. Error bars, ±SD.

diameter than the thin tubules present in wild-type cells (Figures 1, C and D). Similar large tubules were also observed in Δ*mdm10* cells grown at either 23°C or 37°C (Supplementary Figure 2A). Mitochondria in the *N. crassa* strain lacking Tom7 did not resemble mitochondria lacking Mdm10 and even appeared to be slightly thinner than those in wild-type cells (Figures 1, C and D). Mitochondria in the double mutant lacking both Mdm10 and Tom7 appeared to be of intermediate diameter (Figure 1, C and D)—smaller than in the *mdm10* mutant, but larger than in the *tom7* mutant.

Import and Assembly of Precursor Proteins into Mitochondria Lacking Mdm10

We next examined the ability of mitochondria lacking Mdm10 to import and assemble mitochondrial precursor proteins in vitro. Import of the β-subunit of the F_1 ATP synthase ($F_1\beta$, a matrix-targeted precursor) was similar in all the strains examined (Figure 2A). On the other hand, import of the ADP/ATP carrier protein (AAC, an inner membrane–targeted precursor) was reduced in both the *mdm10* mutant and the *mdm10 tom7* double mutant (Figure 2A), although this is likely not due to involvement of Mdm10 in the import of AAC (see below). To determine if *N. crassa* Mdm10 plays a role in the biogenesis of β-barrel proteins, the assembly of the precursor of Tom40 into the TOM (translocase of the outer mitochondrial membrane) complex was examined by BNGE after import into isolated mitochondria. Assembly of Tom40 into the TOM complex occurs through two detectable intermediates (Rapaport and Neupert, 1999; Model *et al.*, 2001; Taylor *et al.*, 2003). With somewhat reduced efficiency in mitochondria lacking Mdm10, the Tom40 precursor was found to reach the first (250 kDa) assembly intermediate, where it is associated with the TOB complex (Figure 2B). Similarly, the precursor was also found in reduced amounts at the second intermediate (100 kDa) where it has been inserted into the membrane by the TOB complex and has associated with preexisting molecules of Tom40 and Tom5 (Model *et al.*, 2001; Wiedemann *et al.*, 2003; Meisinger *et al.*, 2007). Very low amounts of Tom40 precursor were found to assemble into the final TOM complex at 400 kDa in mitochondria lacking Mdm10 (Figure 2B). This suggests that the absence of Mdm10 most strongly affects a post-TOB complex stage of assembly. However, the reduced levels of the intermediates also suggests that the interaction of the TOB complex with the Tom40 precursor may also be affected.

We also examined the assembly of porin, another β-barrel protein. The wild-type control for porin assembly shows four distinct bands after 20–60 min of import (Figure 2C). Although we have not completely defined an assembly pathway for porin in *N. crassa*, we have previously shown that the 240-kDa complex represents the porin precursor in association with the TOB complex (Hoppins *et al.*, 2007). Western blot analysis of mitochondrial proteins after BNGE, shows that most porin is detected in a low-molecular-mass band that corresponds to the 66-kDa band seen on import blots, with minor amounts in the two complexes of ~115 and 170 kDa (unpublished observations). In mitochondria lacking Mdm10 all four bands seen in the wild-type assembly pattern were reduced (Figure 2C). The largest amount of imported precursor was present at 240 kDa, representing an early intermediate associated with the TOB complex (Hoppins *et al.*, 2007), and in the 66-kDa form. The presence of precursor at the 240-kDa intermediate suggests that the effect on the assembly of porin also occurs at least partially at a stage after association with the TOB complex. However, as with Tom40 the amount of precursor at this stage is reduced relative to the control, and interaction of the porin precursor with the TOB complex may not be optimal. Virtually identical results for porin and Tom40 assembly were seen using mitochondria isolated from Δ*mdm10* cells grown at either 23 or 37°C (Supplementary Figure 2B).

The reduction in import of AAC and the difference in effects on porin assembly compared with those reported for *S. cerevisiae* mitochondria lacking Mdm10 prompted us to investigate the possibility that factors other than the absence of Mdm10 were responsible for the observed phenotypes. Because the small Tim complexes (Tim9/10 and Tim8/13) are known to be required for the efficient import of β-barrel proteins (Hoppins and Nargang, 2004; Wiedemann *et al.*, 2004; Habib *et al.*, 2005) and AAC (Curran *et al.*, 2002a,b; Vasiljev *et al.*, 2004; Webb *et al.*, 2006), their loss could have an effect on import and assembly of these proteins. The large size of mitochondria in the mutant strain suggested that they might be more susceptible to damage during the process of isolation. Broken mitochondrial membranes could result in the loss of proteins such as the small Tim complexes from the intermembrane space. Western blot analysis revealed that the levels of the intermembrane space proteins, Tim8 and Tim13, as well as the matrix proteins, Hsp60 and

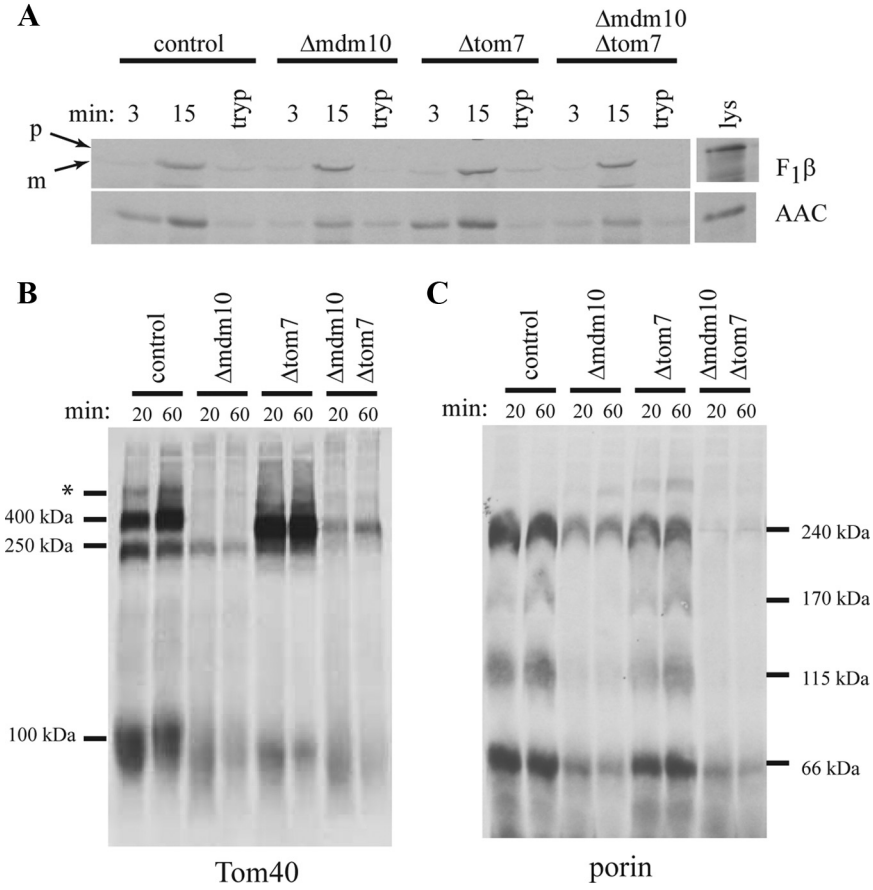

Figure 2. Import of precursor proteins into mitochondria of mutant strains. (A) Import of radiolabeled matrix-targeted β-subunit of mitochondrial F_1 ATP synthase ($F_1\beta$) and the inner membrane targeted ATP/ADP carrier (AAC) into mitochondria isolated from the indicated strains. After import, the mitochondria were treated with proteinase K, reisolated, electrophoresed, transferred to nitrocellulose membranes, and examined by autoradiography. The time (min) of each import reaction is indicated above the lanes. Lys, 33% of the input lysate containing radiolabeled protein used in each reaction; tryp, mitochondria pretreated with trypsin before 8 min of import with precursor protein. For $F_1\beta$, arrows indicate the positions of the precursor (p) and mature (m) forms of the protein. (B) Import of radiolabeled Tom40 precursor into mitochondria isolated from the indicated strains. After import, the mitochondria were reisolated and dissolved in 1% digitonin. The samples were subjected to BNGE, transferred to PVDF membrane, and analyzed by autoradiography. The time (min) of each import reaction is indicated above the lanes. The molecular mass of complexes are indicated in kilodaltons. The asterisk (*) indicates a band previously characterized as a nonproductive intermediate (Taylor *et al.*, 2003). (C) As in B, but radiolabeled porin precursor was imported. The molecular mass of the bands detected in B and C are indicated. The faint bands of highest molecular mass in the Δ*mdm10* and Δ*tom7* lanes appear in some import experiments but not others and have not been characterized.

Hsp70, were reduced in mitochondria isolated from the Δ*mdm10* mutant (Figure 3A). To determine if this was due to loss of these proteins during the isolation procedure, versus an inherently lower level of these proteins in the mutant, we examined whole cell extracts for levels of Tim8 and Tim13. In this case, the levels of the proteins appeared to be similar to those in controls (Figure 3B), supporting the notion that the large mitochondria in Δ*mdm10* mutant cells are physically damaged during isolation. The levels of most other proteins in mitochondria lacking Mdm10 appeared to be similar to those in wild type. Exceptions were Tim23, which is slightly increased in the mutant, as well as Tom40 and Tom22, which appear slightly reduced (Figure 3A).

We wanted to determine if the defects in import and assembly of AAC, Tom40, and porin that were observed in Δ*mdm10* mitochondria were due to lack of Mdm10 or to the decreased levels of intermembrane space and matrix proteins observed to be lost from the mutant mitochondria during isolation. Therefore, we created damaged wild-type mitochondria to act as a control, by subjecting isolated mitochondria to periodic vortexing while in the presence of a hypotonic buffer. Western blot analysis of these damaged wild-type mitochondria showed that the levels of the Tim8, Tim13, and Hsp70 proteins were similar to those in mitochondria isolated from the *mdm10* knockout strain (Figure 4A), whereas the levels of other proteins examined were similar to wild type. Import of the $F_1\beta$ and AAC precursors into the damaged wild-type mitochondria was slightly reduced in comparison to the Mdm10-deficient mitochondria (Figure 4B). This suggests that the inefficient import of AAC in the *mdm10* mutant is likely due to the deficiency of small Tim proteins. The pattern of assembly for the Tom40 precursor into damaged wild-type mitochondria did not resemble the pattern seen in the Mdm10-deficient mitochondria. Although assembly into the final 400-kDa TOM complex in damaged wild-type mitochondria was slightly reduced compared with the wild-type control, it was obviously much more efficient than in the Δ*mdm10* mutant mitochondria (Figure 4C). The presence of the Tom40 precursor at the first two intermediate stages in Mdm10-deficient mitochondria also argues against the import defects being due to reduced levels of the small Tim proteins, as these intermembrane space chaperones are required to guide the incoming precursor to the first intermediate stage (Hoppins and Nargang, 2004; Wiedemann *et al.*, 2004). A similar result was seen for porin where all complexes containing porin were found to be formed more efficiently in the damaged wild-type mitochondria than in those lacking Mdm10 (Figure 4D). We conclude that the lack of Mdm10 is responsible for the majority of the defects relating to Tom40 and porin assembly, whereas the deficiency of the small Tim proteins explains the decrease in AAC import.

Mdm10 and Tom7 Affect Different Steps in the Assembly of β-Barrel Proteins

Previous work in both *N. crassa* and *S. cerevisiae* has shown that mitochondria lacking Tom7 assembled porin less efficiently and Tom40 more efficiently than wild-type mitochondria (Krimmer *et al.*, 2001; Model *et al.*, 2001; Sherman *et al.*, 2005; Meisinger *et al.*, 2006). A model involving a relationship of Mdm10 with Tom7 was proposed to explain these observations in *S. cerevisiae* (Meisinger *et al.*, 2006). To

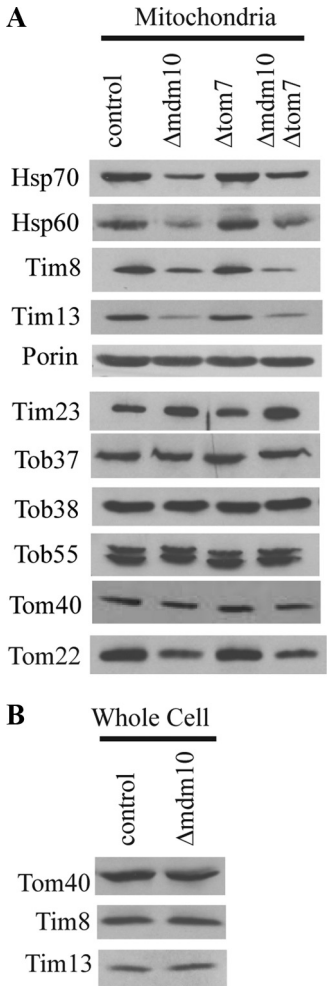

Figure 3. Mitochondrial proteins in mutant strains. (A) Mitochondria (30 μg protein) isolated from the strains indicated were analyzed on Western blots with antibodies to the indicated proteins. (B) Whole cell extracts were prepared from the control (76-26) and *mdm10* knockout strains as described in *Materials and Methods*. The extracts were examined (100 μg protein per lane) using Western blots with antibodies against the indicated proteins.

explore a possible functional relationship of these two proteins in *N. crassa*, we compared the assembly of Tom40 and porin in mitochondria isolated from Δ*tom7* and Δ*mdm10* single and double mutant strains. As reported previously (Sherman *et al.*, 2005), assembly of Tom40 into the final TOM complex occurred more rapidly in mitochondria lacking Tom7, and a TOM complex of slightly smaller size was produced (Figure 2B). However, in mitochondria lacking both Mdm10 and Tom7, assembly of Tom40 to the final 400-kDa form appears to occur less efficiently than in wild-type or Tom7-deficient mitochondria, but more efficiently than in the single Mdm10 mutant (Figure 2B). The final TOM complex in the double mutant has the same size as the single Δ*tom7* mutant. For porin, there was a slight decrease in the formation of all the complexes in mitochondria lacking Tom7, which was less severe than the defects seen in mitochondria lacking Mdm10. However, the defects in porin assembly in the double mutant were greater than in either single mutant (Figure 2C), demonstrating that the deficiencies observed in the single mutants are additive.

Decreased Levels of Assembled TOM Complex in Mitochondria Lacking Mdm10

We were struck by the apparent discrepancy between the almost normal steady-state, carbonate-resistant, levels of Tom40 in the mitochondrial outer membrane of the Δ*mdm10* strain (Figures 1B and 3A), compared with the reduced ability of mitochondria from this strain to assemble the protein to the final TOM complex in vitro (Figure 2B).

It seemed plausible that the steady-state levels of Tom40 observed by Western blot analysis after standard SDS-PAGE might not reflect the amount of the protein actually assembled into a full-sized, functional TOM complex. Lack of Tom40 assembly in vivo could be caused by the absence of Mdm10 and/or the somewhat reduced level of the core TOM complex component, Tom22 (Figure 3A). To test for levels of fully formed TOM complex, we prepared blots after BNGE and decorated these with Tom40 antibodies. Under these conditions it was apparent that mitochondria lacking Mdm10 or both Mdm10 and Tom7 contained a reduced level of TOM complex (Figure 5A, compare lanes with 50 μg mitochondrial protein). To estimate the approximate level of TOM complex in the mutants relative to wild-type mitochondria, we included a dilution series of control mitochondria on the BNGE (Figure 5A). Mitochondria lacking Mdm10 contained ~50% of the control level of TOM complex, whereas the double mutant contained only ~15–20%. Because the amount of Tom40 observed in standard Western blots after SDS-PAGE did not suggest a large difference in the amounts of the protein between the different strains, we expected to see subcomplexes or monomers of Tom40 on the native gels. However, only small amounts of subcomplexes were seen on long exposures (unpublished observations). Conceivably, some Tom40 in the mutants is present in many different forms that do not migrate as one or two discrete bands that are easily detected.

Because there were reduced levels of TOM complex in the mutants, we compared the efficiency of import in the mutants to reduced amounts of control mitochondria. Even when only 5% of the amount of control mitochondria typically present in an import reaction were used, they still imported and assembled Tom40 and porin more efficiently than the mutant mitochondria (Figure 5, B and C). Taken together, these data show that the amount of TOM complex is reduced in the mutants, but the reduction does not account for the deficiencies of β-barrel assembly seen in vitro.

Small Amounts of Mdm10 Are Associated with the TOB Complex

Previous studies have suggested that the TOB holo complex in *S. cerevisiae* arises from an association of Mdm10 with the TOB core complex, consisting of Tob55, Tob38, and Tob37 (Meisinger *et al.*, 2004, 2006). To determine if Mdm10 was associated with the TOB complex in *N. crassa*, we performed affinity binding copurification experiments using strains that express only His-tagged versions of Tob55, Tob38, or Tob37. Isolated mitochondria from each of these strains import Tom40 and porin at rates indistinguishable from wild type (unpublished observations). Mitochondria from each strain were dissolved in digitonin and subjected to Ni-NTA chromatography. Fractions were eluted with imidazole and analyzed by SDS-PAGE and immunodecoration (Figure 6A). For the His-tagged Tob55 strain, each of the three proteins of the TOB core complex was enriched in the elution fraction relative to the amounts in a standard mitochondrial load lane, suggesting a strong association of Tob37 and Tob38 to the His-tagged Tob55. A small amount of porin was also

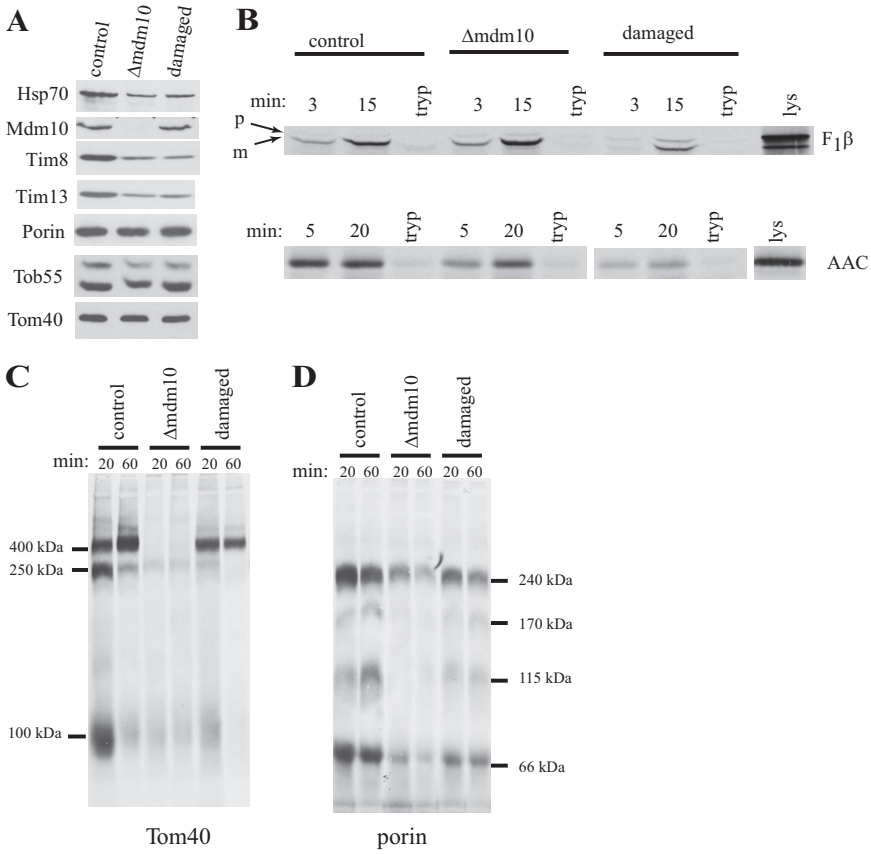

Figure 4. Comparison of mitochondria isolated from the *mdm10* knockout strain and damaged wild-type mitochondria. (A) Mitochondria isolated from the control strain 76-26, the *mdm10* knockout strain, and damaged 76-26 mitochondria (damaged) were compared on Western blots using antibodies directed against the proteins indicated. Each lane contained 30 μg of mitochondrial protein. (B–D) Import of $F_1\beta$ and AAC, Tom40, and porin were as described in the legends to Figures 2, A, B, and C, respectively.

coeluted which may reflect its abundance in the outer membrane. Alternatively, small amounts of porin could coelute as an assembly intermediate trapped in the isolated TOB complex. None of the other outer membrane components examined were detected in the elution with the exception of Mdm10. However, the ratio of Mdm10 in the elution, relative to the amount in the standard lane was many fold lower than the ratio for the Tob core proteins. A virtually identical result was seen when OMV, isolated from His-tagged Tob55 mitochondria, were used as the starting material for the copurification (Supplementary Figure 3). With the tagged Tob37 strain, both Tob37 and Tob38 were enriched several fold in the elution, whereas Tob55 was present at roughly the same level in the standard and elution lanes. Eluted Mdm10 was reduced about two- or threefold, relative to the standard lane. All components of the TOB core complex were enriched several fold when His-tagged Tob38 mitochondria were examined. Although Mdm10 was present in the elution, its enrichment was again many fold lower than the Tob proteins. To quantify the relative fold purification of a Tob core component relative to Mdm10, we prepared a dilution series of the elution fraction from a copurification experiment using the His-tagged Tob37 strain. The dilutions were subjected to SDS-PAGE and Western blot analysis using antibodies to Mdm10 and Tob38 (Figure 6B). Relative to the standard mitochondrial load lane, the amount of Mdm10 in the undiluted elution lane was about twofold decreased. On the other hand, Tob38 was enriched between 5- and 10-fold. Thus, the enrichment of Tob38 over Mdm10 is between 10- and 20-fold. Taken together these data suggest that Mdm10 associates with the TOB complex, but it is present at a much reduced level compared with the core components.

N. crassa *Mitochondria Lacking Mdm12 or Mmm1 Are Deficient in β-Barrel Assembly*

The finding that *N. crassa* mitochondria lacking Mdm10 assembled β-barrel proteins less efficiently made it of interest to determine if removing the other two proteins originally identified as required for maintenance of mitochondrial morphology would have a similar effect. An *N. crassa* mutant in the *mdm12* gene was previously isolated as a hyphal growth morphology mutant (Seiler and Plamann, 2003), and a repeat induced point mutant of the *N. crassa mmm1* gene was previously described as a mitochondrial morphology mutant containing large mitochondrial tubules (Prokisch *et al.*, 2000). We found that mitochondria in the *mdm12* strain existed as large diameter tubules similar to those of the *mdm10* and *mmm1* mutants (Figure 7A). We then examined import of the $F_1\beta$ and AAC precursors into mitochondria isolated from these mutant strains. The pattern of import was similar to that in the *mdm10* mutant with $F_1\beta$ similar to the control and AAC import somewhat reduced (Figure 7B). Again, the large size of these mitochondria suggested that breakage might occur during isolation and, as in the Δ*mdm10* mitochondria, a deficiency of the small Tim proteins and Hsp70 was observed in both mutants (Figure 7C). Other mitochondrial proteins were found at levels similar to those in wild-type. Tom40 assembly in the *mdm12* mutant was found to be deficient, but unlike in mitochondria lacking Mdm10, at least some assembly into the final 400-kDa form was observed (Figure 7D). The assembly of porin resembled the pattern seen in mitochondria lacking Mdm10 (Figure 7D). The assembly of Tom40 and porin was reduced in mitochondria from the *mmm1* mutant (Figure 7E) in a manner similar to mitochondria

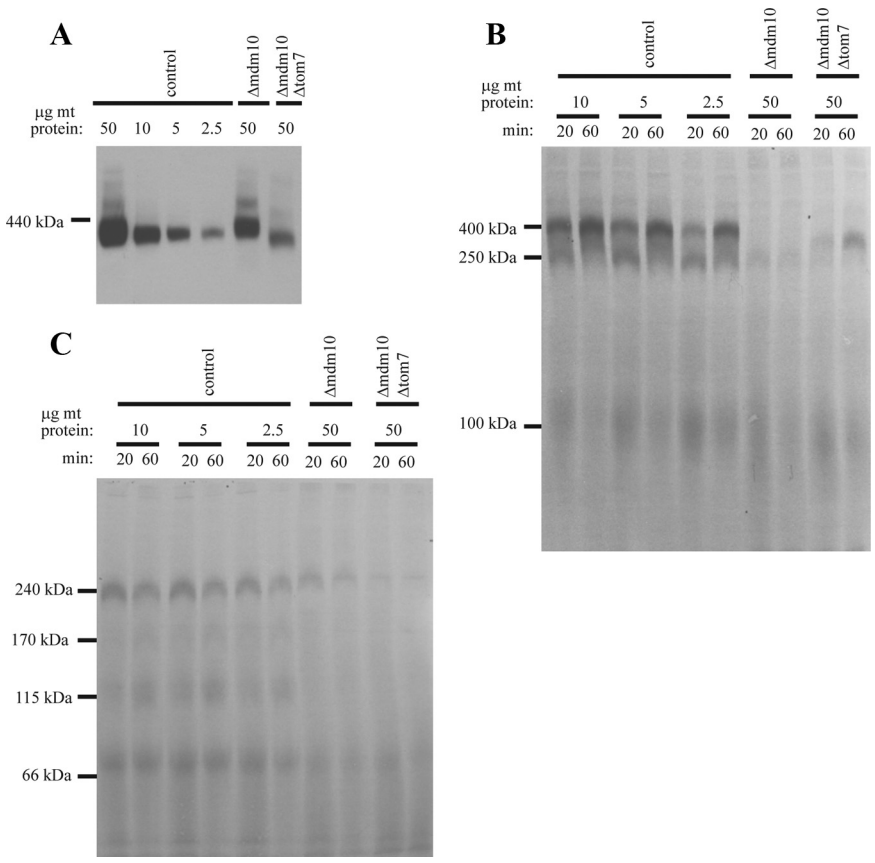

Figure 5. Reduced amounts of TOM complex in strains lacking Mdm10. (A) Mitochondria from the indicated strains were subjected to BNGE, blotted to PVDF membrane, and decorated with Tom40 antibodies. Different amounts of control mitochondria were loaded to allow estimation of the degree of deficiency in the mutants. (B) Import of Tom40 precursor into differing amounts of wild-type mitochondria and standard amounts (50 μg) of mutant mitochondria. Further processing was as described in the legend to Figure 2B. (C) As in B, except that the radiolabeled precursor of porin was imported.

lacking Mdm12. Thus, loss of either the Mdm12 or Mmm1 proteins leads to defects in the assembly of β-barrel proteins in *N. crassa*.

Comparison of growth rates of the three mutants revealed no differences from wild type for the Δ*mdm*10 strain, whereas the *mdm12* mutant has a slight growth defect at 30

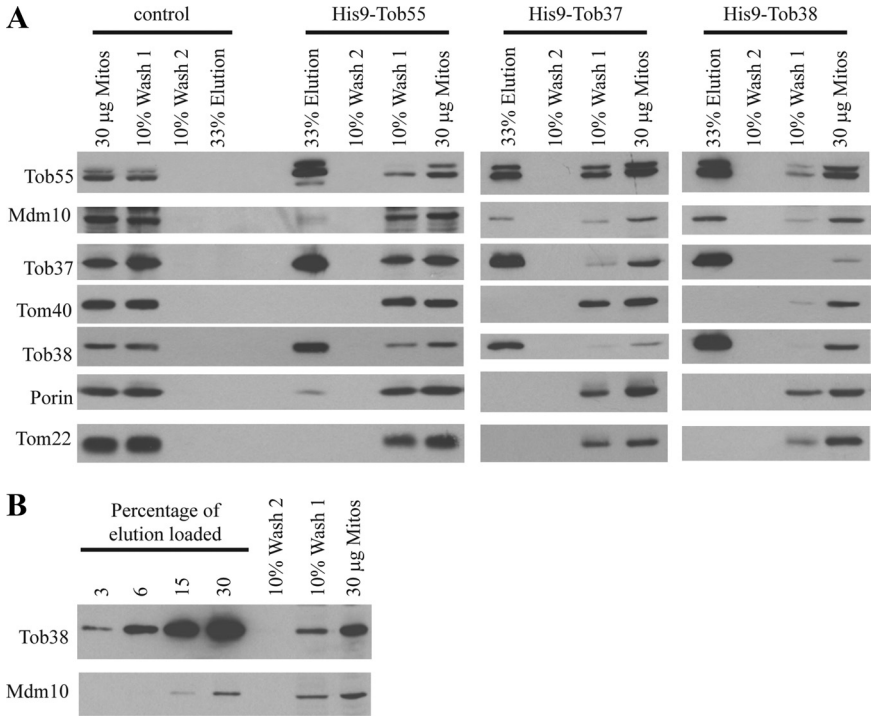

Figure 6. Copurification of outer membrane proteins with TOB core complex components. (A) Mitochondria were isolated from a control strain (76-26) and strains expressing His-tagged versions of Tob37 (His9-Tob37), Tob38 (His9-Tob38), or the isoforms (Hoppins *et al.*, 2007) of Tob55 (His9-Tob55). The mitochondria were solubilized in 1% digitonin in the presence of 50 mM NaCl and 20 mM imidazole. After clarification by centrifugation, the supernatants were bound to Ni-NTA resin and loaded onto columns for affinity purification of Tob proteins and any associated proteins. The column was washed with 10 column volumes of buffer containing 30 mM imidazole and 20 volumes of buffer containing 40 mM imidazole. Elution was performed using 200 mM imidazole. Samples from the indicated fractions were precipitated with trichloroacetic acid and subjected to SDS-PAGE and Western blot analysis using antibodies to the proteins indicated. The lane containing 30 μg of mitochondria serves as a standard to compare relative levels of proteins present in the elution. (B) Comparison of amounts of Tob38 and Mdm10 purified from His9-Tob37 mitochondria. As in A for copurification using His9-Tob37 mitochondria. Dilutions of the elution fraction were also examined to estimate the relative fold purifications of Tob38 and Mdm10.

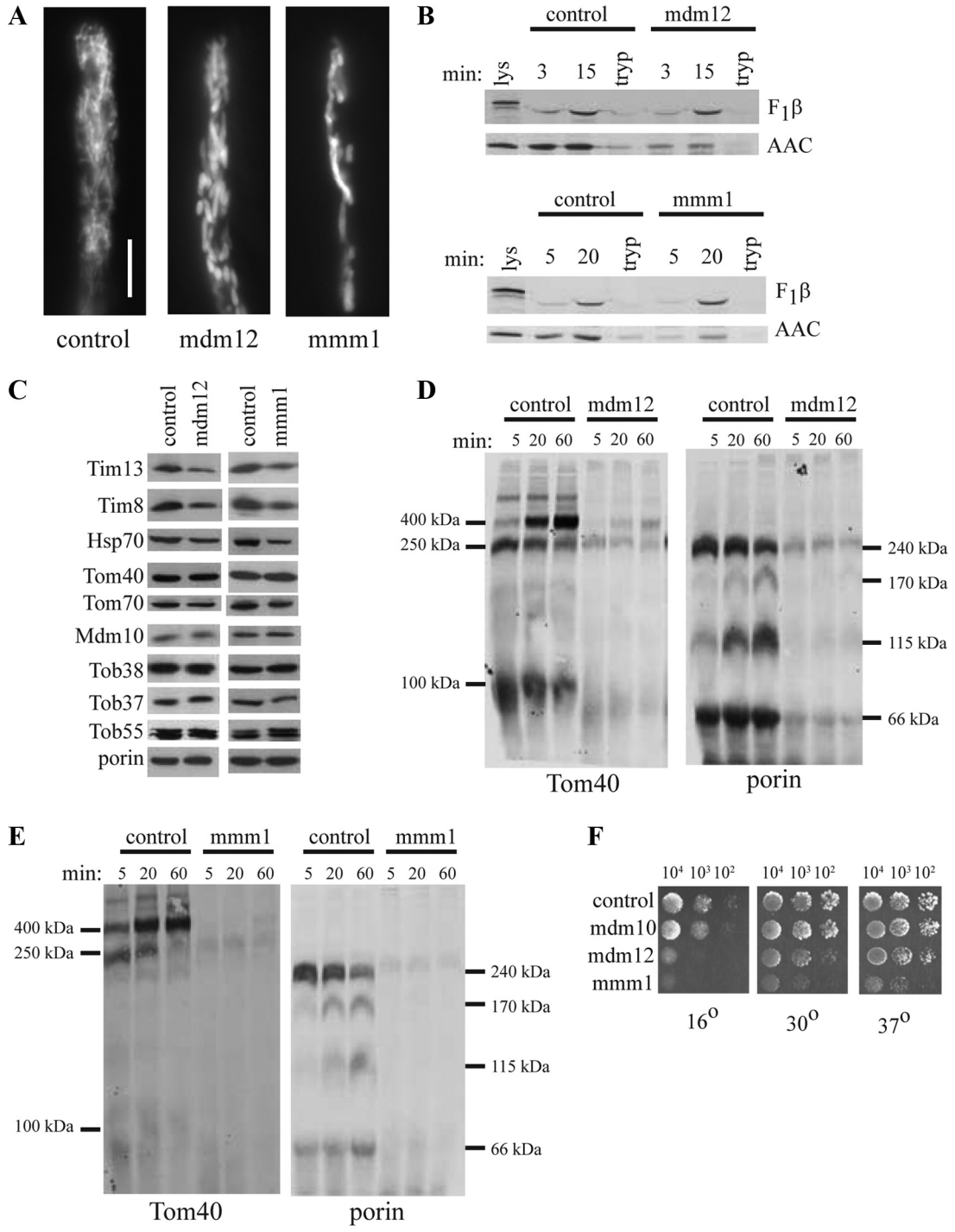

Figure 7. Characterization of mitochondria from *mdm12* and *mmm1* mutants. (A) Hyphae were incubated with MitoTracker Green and examined by fluorescence microscopy. Bar, 10 μm. (B) Precursors of $F_1\beta$ and AAC were imported into mitochondria isolated from the *mdm12* and *mmm1* mutant strains as described in Figure 2. (C) Mitochondrial proteins in the *mdm12* and *mmm1* mutants. Mitochondria were isolated from the indicated strains and subjected to Western blot analysis (30 μg mitochondrial protein per lane) using antibodies directed against the indicated proteins. (D) Import of radiolabeled Tom40 (left) and porin (right) into mitochondria isolated from the *mdm12* mutant as described in the legend to Figure 2. (E) Import of Tom40 (left) and porin (right) into mitochondria isolated from the *mmm1* mutant as described in the legend to Figure 2. (F) Growth rate of mutant strains. Conidiaspores from the control (76-26), and indicated mutant strains were counted and diluted to the desired concentrations. 10^4, 10^3, and 10^2 conidia from each strain were spotted on plates containing Vogel's medium with sorbose. The plates were incubated at 16°C for 72 h, 30°C for 48 h, or 37°C for 48 h and then photographed.

and 37°C, which was exacerbated when grown at 16°C (Figure 7F). As shown previously (Prokisch *et al.*, 2000), the *mmm1* mutant has a more severe growth defect that is apparent at all temperatures examined (Figure 7F). Considering that all these mutants have similar morphological and import characteristics, the severe growth defect of the *mmm1* mutant may indicate additional functions for Mmm1 that are not shared with the other two proteins.

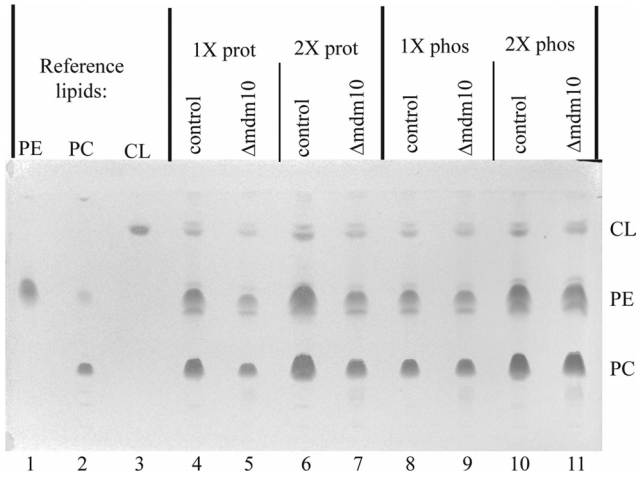

Figure 8. Analysis of mitochondrial outer membrane phospholipids in the Δ*mdm10* mutant. OMV were isolated from either wild-type or Δ*mdm10* mutant cells. Phospholipids were extracted and analyzed by TLC and staining with molybdenum blue. Lane number is indicated at the bottom of the figure. Marker lipids were analyzed in parallel (lanes 1–3). Lanes 4–7, protein concentration in OMVs was measured, and lipids were extracted from samples equivalent to either 270 μg (1X prot) or 540 μg (2X prot) of both wild-type and mutant OMV. Lanes 8–11, Phosphate concentration in OMVs was measured and lipids were extracted from samples equivalent to either 167 μg (1X phos) or 334 μg (2X phos) of both wild-type and mutant OMV. PC, phosphatidylcholine; PE, phosphatidylethanolamine; CL, cardiolipin.

Reduced Phospholipid Levels in Δmdm10 *OMV*

Recently, it has been reported that mitochondria from yeast mutants lacking Mdm10 have altered levels of membrane lipids (Kornmann *et al.*, 2009; Osman *et al.*, 2009), and we wanted to determine if lack of Mdm10 affected lipid composition in the outer membrane of *N. crassa*. Lipids were extracted from OMV and analyzed for their content of the phospholipids phosphatidylcholine (PC), phosphatidylethanolamine (PE), and cardiolipin (CL) by TLC. When extractions were done using OMV from a control and the Δ*mdm10* strain equalized for their level of protein, all three of the phospholipids examined were found to be reduced in the mutant (Figure 8). As a control, for the extraction and analysis, we also examined lipid extracts from control and Δ*mdm10* OMV samples determined to contain equal levels of lipid phosphate. In this case, the levels of phospholipids were comparable in the two strains (Figure 8). When total phosphate levels were determined in the lipids extracted from OMV, the Δ*mdm10* strain was found to contain only ~57% of the wild-type levels of phospholipid when standardized to protein content. We conclude that OMV from the Δ*mdm10* strain are severely altered in their protein to phospholipid ratio.

DISCUSSION

We have shown that *N. crassa* mitochondria lacking either Mdm10, Mdm12, or Mmm1 exist as large diameter tubules and do not efficiently assemble the β-barrel proteins Tom40 and porin into the mitochondrial outer membrane. Absence of any one of the proteins results in decreased formation of all four porin complexes that are observed in assembly assays with wild-type mitochondria. For Tom40 assembly, mitochondria lacking Mdm12 or Mmm1 are deficient in formation of the 250- and 100-kDa intermediates of the assembly pathway, as well as the final 400-kDa TOM complex. In mitochondria lacking Mdm10 the amount of Tom40 assembled into the final 400-kDa TOM complex is more dramatically reduced relative to the reduction in the amount of Tom40 in the intermediates. We also characterized the relationship between Mdm10 and Tom7 in the assembly of Tom40 and porin. *N. crassa* and *S. cerevisiae* mitochondria lacking Tom7 show an increased rate of Tom40 assembly and a decreased ability to assemble porin (Sherman *et al.*, 2005; Meisinger *et al.*, 2006). Here we demonstrate that *N. crassa* mitochondria lacking both Mdm10 and Tom7 show an additive effect of the two single mutations with respect to the assembly of both porin and Tom40. Thus, in the double mutant the rate of incorporation of Tom40 into the TOM complex is intermediate between the low rate in mitochondria lacking Mdm10 and the high rate in mitochondria lacking Tom7. For porin, the inefficient assembly observed in the double *tom7 mdm10* mutant mitochondria is greater than the decrease seen in either single mutant. These results suggest that Mdm10 and Tom7 affect different steps of the assembly pathways for these β-barrel proteins.

Our findings with *N. crassa* differ in several respects from observations in *S. cerevisiae*. For example, mitochondria lacking Mdm10 in *S. cerevisiae* are also inefficient at assembling Tom40 into the final TOM complex but, unlike *N. crassa*, they are more efficient in assembling porin into the outer membrane (Meisinger *et al.*, 2004, 2006). In addition, the *N. crassa* results do not fit with a model developed to explain the assembly patterns of Tom40 and porin in yeast mitochondria lacking either Mdm10 or Tom7 (Meisinger *et al.*, 2006). The basis of the model for *S. cerevisiae* is the existence of two forms of the TOB complex: a holo TOB complex containing Mdm10 that favors assembly of Tom40 and a core TOB complex without Mdm10 that favors porin assembly. The equilibrium between the two forms is thought to be influenced by Tom7, which was shown to be capable of forming a complex with Mdm10 (Meisinger *et al.*, 2006). Thus, in wild-type mitochondria, Tom7 would sequester a certain amount of Mdm10 and the ratio of the two forms of the TOB complex would be maintained at a standard level. However, in mitochondria lacking Tom7 the normally sequestered population of Mdm10 would be available for other interactions resulting in an increase in the level of the holo TOB complex and a decrease in the level of the core TOB complex. Examination of this model suggests that the import phenotype of a Δ*mdm10* Δ*tom7* double mutant should not differ from the single Δ*mdm10* mutant, because in both cases the level of holo TOB complex would be reduced to a similar extent due to lack of Mdm10. However, as described above, our results with *N. crassa* clearly show that mitochondria lacking both Mdm10 and Tom7 assemble Tom40 and porin in a manner that suggests the effects of the two mutations are additive.

We previously suggested a model to explain the assembly of Tom40 and porin in mutants of *N. crassa* lacking Tom7 (Sherman *et al.*, 2005). Newly imported Tom40 subunits might simply be incorporated into the TOM complex more easily in mitochondria lacking Tom7 because loss of the protein results in decreased complex stability (Sherman *et al.*, 2005) and assembly of new subunits into the TOM complex occurs by replacement of existing subunits (Rapaport and Neupert, 1999; Model *et al.*, 2001; Rapaport *et al.*, 2001). Decreased porin import was suggested to be due to a specific role of Tom7 in the import or assembly of the porin precursor. To incorporate our current findings into this model, we suggest that lack of Mdm10 results in a general effect on the function of the TOB complex, which is manifested in a reduced rate of incorporation of β-barrel precur-

sors into the membrane. Because the amount of Tom40 precursor that reaches the final TOM complex is most seriously affected, it is conceivable that some of the molecules put into the membrane by the compromised TOB complex in the absence of Mdm10 are improperly inserted so that fewer precursors exist in the correct conformation to complete the assembly pathway. Loss of Mdm12 or Mmm1 may also result in general defects of TOB complex function.

Further differences between *N. crassa* and *S. cerevisiae* were also noted. Mitochondria in *N. crassa* Δ*tom7* cells, resemble those in wild-type cells and may even be slightly thinner than the wild-type tubules. In *S. cerevisiae*, mitochondria lacking Tom7 are enlarged and unevenly distributed in cells (Dimmer *et al.*, 2002; Meisinger *et al.*, 2006). Interestingly, the effects of Tom7 depletion in human cells more closely resemble those in *N. crassa* with respect to TOM complex stability and mitochondrial morphology (Kato and Mihara, 2008). The growth phenotypes of the *N. crassa mdm10*, *mdm12*, and *mmm1* mutants are generally less severe than those seen in the corresponding yeast mutants. This may be due to the effects the mutations have on mitochondrial distribution in yeast (Burgess *et al.*, 1994; Sogo and Yaffe, 1994; Berger *et al.*, 1997), where a daughter cell must receive a mitochondrion to ensure its survival. The coenocytic nature and hyphal extension growth character of *N. crassa* may mitigate possible effects on mitochondrial distribution because growth of the mycelium does not involve formation of new free living daughter cells or cellular compartments.

As in *S. cerevisiae* (Meisinger *et al.*, 2004, 2007), our data show an association of Mdm10 with the TOB complex. However, the amount of Mdm10 present is much less than any of the TOB core components, and association of Mdm10 with the complex appears to be substoichiometric. It is possible that the association of Mdm10 with the TOB complex might be relatively weak so that the protein is lost during the copurification procedure. Alternatively, only a small subset of TOB complexes may contain Mdm10. It is also conceivable that the low level of Mdm10 observed to be associated with the TOB complex represents assembly intermediates of the protein trapped at the TOB complex during isolation.

Our results clearly show that *N. crassa* cells lacking either Mdm10, Mdm12, or Mmm1 contain mitochondria with altered morphology that are unable to efficiently assemble porin and Tom40 into the outer membrane. However, virtually nothing is known about the actual mechanism of action of these proteins and how the disruption of their function gives rise to multiple phenotypes. Mdm10 has been the most actively studied of the three proteins, and in *S. cerevisiae* it has been shown to have a variety of interactions including association with the TOB complex, binding to Tom7, and formation of the MDM complex with Mdm12 and Mmm1. Each of these interactions may explain aspects of the phenotypes observed in strains lacking Mdm10. On the other hand, in *N. crassa*, genetic evidence suggests that there may not be an interaction between Tom7 and Mdm10 and perhaps only a marginal interaction between Mdm10 and the TOB complex. Thus, some of the observed phenotypes may be secondary effects that result from loss of a single primary function. We have shown that OMV from mitochondria lacking Mdm10 in *N. crassa* are deficient in PC, PE, and CL. One possibility for the primary function of Mdm10 might be its role in the formation of the complex that forms contacts between mitochondria and the ER (Kornmann *et al.*, 2009). The complex is thought to be important for lipid and calcium exchange between the two organelles and alterations in phospholipid metabolism or content have been shown in *S. cerevisiae* cells lacking Mdm10, Mdm12, or Mmm1 (Kornmann *et al.*, 2009; Osman *et al.*, 2009). Furthermore, Mdm10 and Mmm1 were identified in a screen for genetic interactors of prohibitins, proteins thought to be responsible for the organization of proteins and lipids of the inner mitochondrial membrane (Osman *et al.*, 2009). Alterations in membrane lipid composition are known to have effects on the topogenesis of membrane proteins (Dowhan and Bogdanov, 2009), and several reports have described alterations in mitochondrial membrane protein function as the result of changes in lipid composition. For example, changes in CL levels have been shown to affect the assembly and activity of AAC and the TIM23 complex (Jiang *et al.*, 2000; Kutik *et al.*, 2008; Claypool, 2009; Klingenberg, 2009; Tamura *et al.*, 2009). Furthermore, it has recently been demonstrated that the activities of the TOM and TOB complexes are altered in mutants affecting CL synthesis (Gebert *et al.*, 2009). Altered lipid composition might also affect mitochondrial morphology. Much more work will be required to define the precise functions and mechanisms of action of Mdm10, Mdm12, and Mmm1 and to distinguish between primary and secondary phenotypic effects observed in mutants.

ACKNOWLEDGMENTS

We are grateful to Enrico Scarpella for the use of his fluorescence microscope and for his instruction regarding the use of the instrument. We thank Colin Lin for technical assistance. J.G.W. was supported by a post-graduate scholarship from the National Sciences and Engineering Research Council. This work was supported by a grant from the Canadian Institutes of Health Research to F.E.N. and grants from the Deutsche Forschungsgemeinschaft to D.R. and W.N.

REFERENCES

Becker, T., Gebert, M., Pfanner, N., and van der Laan, M. (2009). Biogenesis of mitochondrial membrane proteins. Curr. Opin. Cell Biol. *21*, 484–493.

Becker, T., Vögtle, F.-N., Stojanovski, D., and Meisinger, C. (2008). Sorting and assembly of mitochondrial outer membrane proteins. Biochim. Biophys. Acta *1777*, 557–563.

Berger, K. H., Sogo, L. F., and Yaffe, M. P. (1997). Mdm12p, a component required for mitochondrial inheritance that is conserved between budding and fission yeast. J. Cell Biol. *136*, 545–553.

Boldogh, I. R., Nowakowski, D. W., Yang, H.-C., Chung, H., Karmon, S., Royes, P., and Pon, L. A. (2003). A protein complex containing Mdm10p, Mdm12p, and Mmm1p links mitochondrial membranes and DNA to the cytoskeleton-based segregation machinery. Mol. Biol. Cell *14*, 4618–4627.

Bolender, N., Sickmann, A., Wagner, R., Meisinger, C., and Pfanner, N. (2008). Multiple pathways for sorting mitochondrial precursor proteins. EMBO Rep. *9*, 42–49.

Böttcher, C.J.F., van Gent, C. M., and Pries, C. (1961). A rapid and sensitive sub-micro phosphorus determination. Anal. Chim. Acta *24*, 203–204.

Burgess, S. M., Delannoy, M., and Jensen, R. E. (1994). MMM1 encodes a mitochondrial outer membrane protein essential for establishing and maintaining the structure of yeast mitochondria. J. Cell Biol. *126*, 1375–1391.

Chacinska, A., Koehler, C., Milenkovic, D., Lithgow, T., and Pfanner, N. (2009). Importing mitochondrial proteins: machineries and mechanisms. Cell *138*, 628–644.

Claypool, S. M. (2009). Cardiolipin, a critical determinant of mitochondrial carrier protein assembly and function. Biochim. Biophys. Acta *1788*, 2059–2068.

Curran, S. P., Leuenberger, D., Oppliger, W., and Koehler, C. M. (2002a). The Tim9p-Tim10p complex binds to the transmembrane domains of the ADP/ATP carrier. EMBO J. *21*, 942–953.

Curran, S. P., Leuenberger, D., Schmidt, E., and Koehler, C. M. (2002b). The role of the Tim8p-Tim13p complex in a conserved import pathway for mitochondrial polytopic inner membrane proteins. J. Cell Biol. *158*, 1017–1027.

Davis, R. H., and De Serres, F. J. (1970). Genetic and microbiological research techniques for *Neurospora crassa*. Methods Enzymol. *17*, 79–143.

Dimmer, K.S., Fritz, S., Fuchs, F., Messerschmitt, M., Weinbach, N., Neupert, W., and Westermann, B. (2002). Genetic basis of mitochondrial function and morphology in *Saccharomyces cerevisiae*. Mol. Biol. Cell *13*, 847–853.

Dowhan, W., and Bogdanov, M. (2009). Lipid-dependent membrane protein topogenesis. Annu. Rev. Biochem. *78*, 515–540.

Galagan, J. E., *et al*. (2003). The genome sequence of the filamentous fungus *Neurospora crassa.* Nature *422*, 859–868.

Gebert, N., *et al*. (2009). Mitochondrial cardiolipin involved in outer-membrane protein biogenesis: implications for Barth syndrome. Curr. Biol. *19*, 1–7.

Good, A. G., and Crosby, W. L. (1989). Anaerobic induction of alanine aminotransferase in barley root tissue. Plant Physiol. *90*, 1305–1309.

Habib, S. J., Waizenegger, T., Lech, M., Neupert, W., and Rapaport, D. (2005). Assembly of the TOB complex of mitochondria. J. Biol. Chem. *280*, 6434–6440.

Harkness, T.A.A., Nargang, F. E., Van der Klei, I., Neupert, W., and Lill, R. (1994). A crucial role of the mitochondrial protein import receptor MOM19 for the biogenesis of mitochondria. J. Cell Biol. *124*, 637–648.

Hickey, P. C., Swift, S. R., Roca, M. G., and Read, N. D. (2005). Live-cell imaging of filamentous fungi using vital fluorescent dyes and confocal microscopy. In: Methods in Microbiology, Vol. *34*, Microbial Imaging, ed. T. Savidge, and C. Pothulakis, London: Elsevier, 63–87.

Hoppins, S. C., Go, N. E., Klein, A., Schmitt, S., Neupert, W., Rapaport, D., and Nargang, F. E. (2007). Alternative splicing gives rise to different isoforms of the *Neurospora crassa* Tob55 protein that vary in their ability to insert β-barrel proteins into the outer mitochondrial membrane. Genetics *177*, 137–149.

Hoppins, S. C., and Nargang, F. E. (2004). The Tim8-Tim13 complex of *Neurospora crassa* functions in the assembly of proteins into both mitochondrial membranes. J. Biol. Chem. *279*, 12396–12405.

Ishikawa, D., Yamamoto, H., Tamura, Y., Moritoh, K., and Endo, T. (2004). Two novel proteins in the mitochondrial outer membrane mediate β-barrel protein assembly. J. Cell Biol. *166*, 621–627.

Jamet-Vierny, C., Contamine, V., Boulay, J., Zickler, D., and Picard, M. (1997). Mutations in genes encoding the mitochondrial outer membrane proteins Tom70 and Mdm10 of *Podospora anserina* modify the spectrum of mitochondrial DNA rearrangements associated with cellular death. Mol. Cell. Biol. *17*, 6359–6366.

Jiang, F., Ryan, M. T., Schlame, M., Zhao, Z., Gu, Z., Klingenberg, M., Pfanner, N., and Greenberg, M. L. (2000). Absence of cardiolipin in the *crd1* null mutant results in decreased mitochondrial membrane potential and reduced mitochondrial function. J. Biol. Chem. *275*, 22387–22394.

Kato, H., and Mihara, K. (2008). Identification of Tom5 and Tom6 in the preprotein translocase complex of human mitochondrial outer membrane. Biochem. Biophys. Res. Comm. *369*, 958–963.

Klingenberg, M. (2009). Cardiolipin and mitochondrial carriers. Biochim. Biophys. Acta *178*, 2048–2058.

Koch, K. V., Suelmann, R., and Fischer, R. (2003). Deletion of *mdmB* impairs mitochondrial distribution and morphology in *Aspergillus nidulans*. Cell Motil. Cytoskelet. *55*, 114–124.

Kornmann, B., Currie, E., Collins, S. R., Schuldiner, M., Nunnari, J., Weissman, J. S., and Walter, P. (2009). An ER-mitochondria tethering complex revealed by a synthetic biology screen. Science *325*, 477–481.

Krimmer, T., *et al.* (2001). Biogenesis of porin of the outer mitochondrial membrane involves an import pathway via receptors and the general import pore of the TOM complex. J. Cell Biol. *152*, 289–300.

Kutik, S., *et al.* (2008). The translocator maintenance protein Tam41 is required for mitochondrial cardiolipin biosynthesis. J. Cell Biol. *183*, 1213–1221.

Lueder, F., and Lithgow, T. (2009). The three domains of the mitochondrial outer membrane protein Mim1 have discrete functions in assembly of the TOM complex. FEBS Lett. *583*, 1475–1480.

Mayer, A., Driessen, A., Neupert, W., and Lill, R. (1995). Purified and protein-loaded mitochondrial outer membrane vesicles for functional analysis of preprotein transport. Methods Enzymol. *260*, 252–263.

Meisinger, C., *et al.* (2007). The morphology proteins Mdm12/Mmm1 function in the major β-barrel assembly pathway of mitochondria. EMBO J. *26*, 2229–2239.

Meisinger, C., *et al.* (2004). The mitochondrial morphology protein Mdm10 functions in assembly of the preprotein translocase of the outer membrane. Dev. Cell *7*, 61–71.

Meisinger, C., Wiedemann, N., Rissler, M., Strub, A., Milenkovic, D., Schönfisch, B., Müller, H., Kozjak, V., and Pfanner, N. (2006). Mitochondrial protein sorting: differentiation of β-barrel assembly by Tom7-mediated segregation of Mdm10. J. Biol. Chem. *281*, 22819–22826.

Model, K., Meisinger, C., Prinz, T., Wiedemann, N., Truscott, K. N., Pfanner, N., and Ryan, M. T. (2001). Multistep assembly of the protein import channel of the mitochondrial outer membrane. Nat. Struct. Biol. *8*, 361–370.

Nargang, F. E., and Rapaport, D. (2007). *Neurospora crassa* as a model organism for mitochondrial biogenesis. In: Mitochondria. Practical Protocols, eds. D.L. Leister and J. Herrmann, Totowa, NJ: Humana Press.

Neupert, W., and Herrmann, J. (2007). Translocation of proteins into mitochondria. Annu. Rev. Biochem. *76*, 723–749.

Osman, C., Haag, M., Potting, C., Rodenfels, J., Dip, P. V., Wieland, F. T., Brügger, B., Westermann, B., and Langer, T. (2009). The genetic interactome of prohibitins: coordinated control of cardiolipin and phosphatidylethanolamine by conserved regulators in mitochondria. J. Cell Biol. *184*, 583–596.

Prokisch, H., Neupert, W., and Westermann, B. (2000). Role of MMM1 in maintaining mitochondrial morphology in *Neurospora crassa.* Mol. Biol. Cell *11*, 2961–2971.

Rapaport, D., and Neupert, W. (1999). Biogenesis of Tom40, core component of the TOM complex of mitochondria. J. Cell Biol. *146*, 321–331.

Rapaport, D., Taylor, R., Käser, M., Langer, T., Neupert, W., and Nargang, F. E. (2001). Structural requirements of Tom40 for assembly into preexisting TOM complexes of mitochondria. Mol. Biol. Cell *12*, 1189–1198.

Schägger, H., Cramer, W. A., and von Jagow, G. (1994). Analysis of molecular masses and oligomeric states of protein complexes by blue native electrophoresis and isolation of membrane protein complexes by two-dimensional native electrophoresis. Anal. Biochem. *217*, 220–230.

Schägger, H., and von Jagow, G. (1991). Blue native electrophoresis for isolation of membrane complexes in enzymatically active form. Anal. Biochem. *199*, 223–231.

Seiler, S., and Plamann, M. (2003). The genetic basis of cellular morphogenesis in the filamentous fungus *Neurospora crassa.* Mol. Biol. Cell *14*, 4352–4364.

Sherman, E. L., Go, N. E., and Nargang, F. E. (2005). Functions of the small proteins in the TOM complex of *Neurospora crassa.* Mol. Biol. Cell *16*, 4172–4182.

Sogo, L. F., and Yaffe, M. P. (1994). Regulation of mitochondrial morphology and inheritance by Mdm10p, a protein of the mitochondrial outer membrane. J. Cell Biol. *126*, 1361–1373.

Tamura, Y., Endo, T., Lijima, M., and Sesaki, H. (2009). Ups1p and Ups2p antagonistically regulate cardiolipin metabolism in mitochondria. J. Cell Biol. *185*, 1029–1045.

Taylor, R., McHale, B., and Nargang, F. E. (2003). Characterization of *Neurospora crassa* Tom40-deficient mutants and effect of specific mutations on Tom40 assembly. J. Biol. Chem. *278*, 765–775.

Vaden, D. L., Gohil, V. M., Gu, Z., and Greenberg, M. L. (2005). Separation of yeast phospholipids using one-dimensional thin-layer chromatography. Anal. Biochem. *338*, 162–164.

Vasiljev, A., *et al.* (2004). Reconstituted TOM core complex and Tim9/Tim10 complex of mitochondria are sufficient for translocation of the ADP/ATP carrier across membranes. Mol. Biol. Cell *15*, 1445–1458.

Waizenegger, T., Schmitt, S., Zivkovic, J., Neupert, W., and Rapaport, D. (2005). Mim1, a protein required for the assembly of the TOM complex of mitochondria. EMBO Rep. *6*, 57–62.

Walther, D.M., Rapaport, D., and Tommassen, J. (2009). Biogenesis of beta-barrel membrane proteins in bacteria and eukaryotes: evolutionary conservation and divergence. Cell. Mol. Life Sci. *66*, 2789–2804.

Webb, C. T., Gorman, M. A., Lazarou, M., Ryan, M. T., and Gulbis, J. M. (2006). Crystal structure of the mitochondrial chaperone TIM9–10 reveals a six-bladed α-propeller. Mol. Cell *21*, 123–133.

Wiedemann, N., Kozjak, V., Chacinska, A., Schönfisch, B., Rospert, S., Ryan, M. T., Pfanner, N., and Meisinger, C. (2003). Machinery for protein sorting and assembly in the mitochondrial outer membrane. Nature *424*, 565–571.

Wiedemann, N., Truscott, K. N., Pfannschmidt, S., Guiard, B., Meisinger, C., and Pfanner, N. (2004). Biogenesis of the protein import channel Tom40 of the mitochondrial outer membrane. Intermembrane space components are involved in an early stage of the assembly pathway. J. Biol. Chem. *279*, 18188–18194.